



# Molecular simulations of benzene and hexafluorobenzene using new optimized effective potential models: Investigation of the liquid, vapor–liquid coexistence and supercritical fluid phases

Dimitris Dellis\*, Ioannis Skarmoutsos, Jannis Samios

Physical Chemistry Laboratory, Department of Chemistry, University of Athens, Panepistimiopolis 15771, Athens, Greece

## ARTICLE INFO

Available online 8 May 2009

### Keywords:

Benzene  
Hexafluorobenzene  
Supercritical  
Local density inhomogeneities  
Force field  
Molecular dynamics  
Monte Carlo

## ABSTRACT

The development of new effective intermolecular potential models of benzene and hexafluorobenzene, capable in reproducing the thermodynamic and structural properties of molecular systems in a wide range of thermodynamic state points has been presented and discussed. Subsequently, the properties of the fluids have been investigated by employing molecular dynamics and Monte Carlo simulation techniques. The main purpose of this study was to reveal information concerning the liquid state, vapor–liquid equilibrium and supercritical phase properties of these fluids. In the case of the supercritical phase, we mainly focused on the behavior of local density inhomogeneities and related properties. Our calculations reveal that the local density augmentation is much more pronounced in the case of hexafluorobenzene. The origins of possible resemblances and discrepancies with available experimental data have been also systematically discussed and related to our conclusions reported in previous publications. The local density reorganization dynamics as a function of the bulk density and the size of the local region have been also studied, revealing a significant density and length scale dependence similar to the ones presented for other pure supercritical fluids in previous publication of our group.

© 2009 Elsevier B.V. All rights reserved.

## 1. Introduction

It is widely accepted nowadays that molecular simulation is one of the most powerful tools in predicting a wide range of properties of fluid systems, exhibiting thus very significant applications in chemistry, physics, materials science and biology [1–3]. Up to now, the majority of the scientific community is mainly using classical molecular simulation techniques (molecular dynamics or Monte Carlo) to investigate fluid phase properties. An extensive presentation of methods and techniques employed to study all these properties by classical molecular simulation can be found in many books and review articles [1–3] and refs therein. A key point on fluid phase classical molecular simulation is the selection of the appropriate molecular force fields, in order to provide a more realistic description of fluid properties in a wide range of thermodynamic conditions. It is common knowledge that the majority of the existing force fields have been parameterized to describe mainly liquid state properties and their transferability in different fluid phases has not been widely tested. Therefore the development of methods which ensure, more or less, the transferability of classical force fields in several fluid phases becomes indispensable.

One additional and very important reason for this is also the necessity to provide realistic force fields to investigate the properties of condensed matter systems exhibiting some peculiar characteristic properties usually observed in much more extreme thermodynamic conditions than the ambient ones. A characteristic example of such type of fluids is the case of supercritical fluids (SC) and their mixtures (e.g. with ionic liquids). SC fluids represent one of the most interesting categories of solvents used in a wide range of applications in several fields like green chemistry, materials science, engineering etc [4–6]. For this reason, especially the last two decades, many research groups have focused their attention on the properties of SC fluids and many publications and reviews have been devoted to their special characteristics. According to the literature many interesting properties of SC fluids, like their high compressibility values in the near-critical region, have been attributed to some peculiar structural effects occurring in these fluids. It is widely known now that the structure of a SC fluid does not resemble that one of a homogeneous fluid and significant density inhomogeneities may be observed [6]. These distinct fluctuations in density are maximized in the thermodynamic phase region close to the critical point, causing a corresponding maximization of the isothermal compressibility factor  $k_T$ . A systematic investigation of these important phenomena occurring in SC fluids might shed some light on many open questions upon their special characteristics, and molecular simulation is one of the most appropriate techniques to do so. Therefore, the importance of developing

\* Corresponding author.

E-mail address: [ntell@chem.uoa.gr](mailto:ntell@chem.uoa.gr) (D. Dellis).

force fields which provide accurately the thermodynamic, structural and dynamic properties of molecular systems in the SC phase, as well as in vapor–liquid equilibrium state points, become unambiguous.

In our previous studies [7–9], we have started a systematic investigation of local density inhomogeneities and related properties in a wide range of SC solvents. In these works we have focused on the static and dynamic behavior of local density inhomogeneities and on the effect of the nature of intermolecular interactions on these static and dynamic properties. The results obtained so far have revealed a significant influence of the polarity and hydrogen bonding on the extent of local density augmentation in SC fluids. Moreover, our results have shown that the dynamic behavior of the local density is significantly affected by the bulk density of the system and by the size of the local region. Specifically, we have revealed a different density dependence of the calculated local density reorganization times corresponding to short and larger space regions around a tagged central molecule, respectively.

In the present treatment, we have focused our attention on the investigation of this type of properties, amongst others, for fluid benzene and hexafluorobenzene. Initially, in order to simulate these fluid systems we employed some previously proposed in the literature potential models [10–12]. However, our calculations revealed that the previously proposed potential models fail to reproduce several properties of the fluids, especially at higher temperatures and pressures. Therefore, to provide a most accurate description of the thermodynamic, structural and dynamic properties of  $C_6H_6$  and  $C_6F_6$

in a wide range of thermodynamic conditions we developed two new potential models for these systems, based on a systematic optimization procedure. Afterwards, using these newly developed potentials we calculated the above mentioned properties of the fluids and the results obtained are presented and discussed.

The paper is organized as follows: in Section 2 the development and evaluation of the new potential models, as well as the computational details of the simulations are presented. The results and discussion concerning the investigation of local density inhomogeneities and related properties in SC  $C_6H_6$  and  $C_6F_6$  are presented in Section 3 and finally the concluding remarks of our study are summarized in Section 4.

## 2. Potential models optimization and evaluation

As mentioned in the Introduction section, we initially employed in our treatment available potential models for benzene and hexafluorobenzene, namely the OPLS [10] and the ones proposed by Cabaco et al. [11]. In order to examine the accuracy of these models in predicting the pressure of the systems, especially at thermodynamic conditions where the accurate calculation of pressure and density is a very important factor, we performed trial simulation runs at a representative SC isotherm. The results obtained are presented in Fig. 1a, where we observe that the previously proposed models systematically overestimate the system pressure. Trial runs at additional liquid and SC

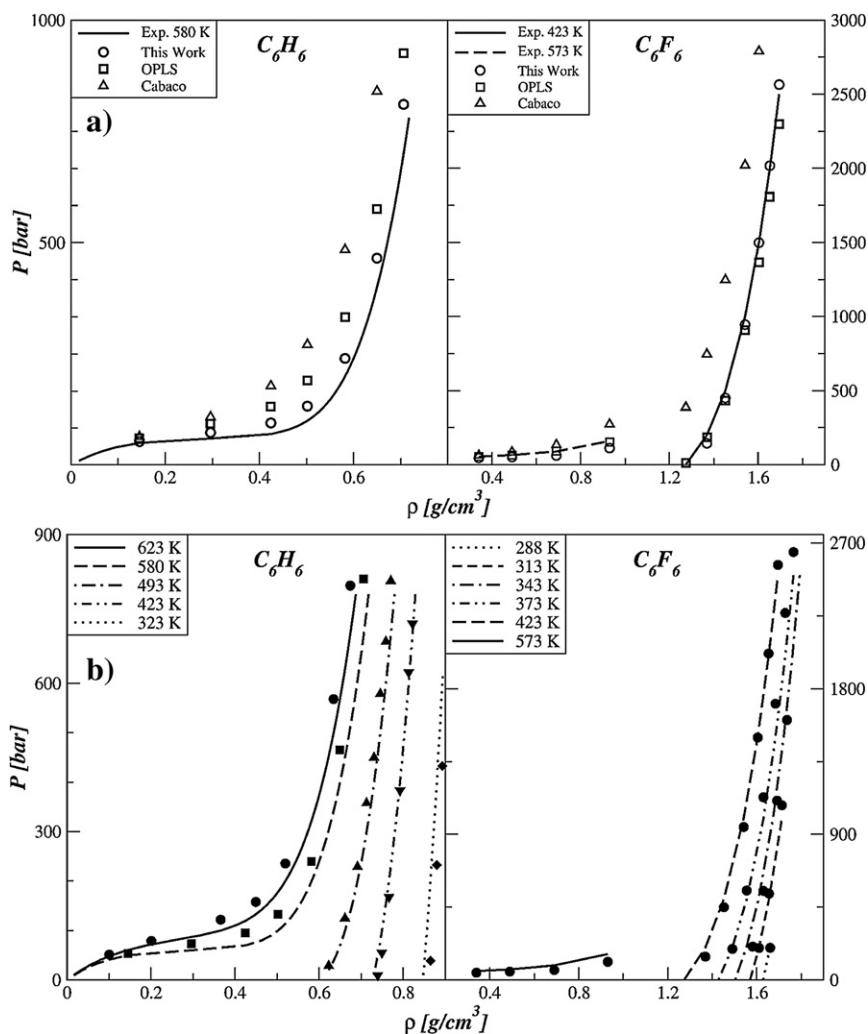


Fig. 1. a) The experimental (lines) [14,15] and simulated pressure of  $C_6H_6$  and  $C_6F_6$  using the potential model of this work (circles), OPLS (squares) and Cabaco (triangles) at SC isotherms. b) Comparison between simulated (closed symbols) and experimental pressure (lines) using the proposed in this work potential models for  $C_6H_6$  [14] and  $C_6F_6$  [15].

conditions have also showed that the deviation between calculated and experimental pressure increases with temperature.

Therefore, to provide a most accurate description of the properties of the systems, we applied a potential optimization method. The potential optimization method includes the minimization of the deviation between simulated and experimental pressure at a wide range of density and temperature state points including liquid, vapor and supercritical regions. In order to perform this optimization procedure, we employed a rigid, all atom description using site–site Lennard–Jones (LJ) and coulombic interactions of the form:

$$U = \sum_{i=1}^{12} \sum_{j=1}^{12} 4\epsilon_{ij} \left[ \left( \frac{\sigma_{ij}}{r_{ij}} \right)^{12} - \left( \frac{\sigma_{ij}}{r_{ij}} \right)^6 \right] + \frac{1}{4\pi\epsilon_0} \frac{q_i q_j}{r_{ij}} \quad (1)$$

The cross interactions are described by the Lorentz–Berthelot combining rule. The selected molecular geometries for benzene and hexafluorobenzene were adopted from ref. [11] since they correspond to the experimental ones. The charge distributions were also taken from the same reference, where they were obtained by ab-initio calculations. In our treatment we focused on the optimization of the LJ van der Waals parameters. The key factor in this optimization procedure was to reproduce the experimental pressure in a wide range of PVT state points using Molecular Dynamics (MD) simulations. This optimization was performed at thermodynamic conditions where experimental data are available [13]. In the case of benzene we selected five isotherms at 323, 423, 493, 580 and 623 K and we optimized the  $\epsilon$  and  $\sigma$  parameters for C and H atoms. In the case of hexafluorobenzene the available experimental data are restricted only in a limited range of P,V,T state points [14,15]. Taking this into account, and in order to propose also a systematic description of a force field for benzene-like molecules, we adopted the same  $\epsilon$  and  $\sigma$  parameters of C atom as in the case of benzene and then optimized the  $\epsilon$  and  $\sigma$  parameters of the F atom, to reproduce the experimental pressures along six isotherms in the range 288–423 [14] and 573 K [15]. The  $\epsilon$  and  $\sigma$  parameters for C, H and F atoms obtained applying this procedure as well as the charges and bond lengths from literature [11] are presented in Table 1. All MD simulations for potential optimization were performed with Gromacs [16] using 343 rigid molecules in the NVT ensemble, with a time step of 2 fs. The equilibration period of each run was 50 ps followed by a subsequent 200 ps optimization run.

The efficiency of the newly developed potential models in reproducing the experimental pressure at a wide range of thermodynamic state points, corresponding to liquid and SC conditions has been

**Table 1**  
Optimized intermolecular potential model parameters and the predicted critical temperature, density and pressure together with the corresponding experimental data.

		Benzene	Hexafluorobenzene
$\epsilon_C/k_B$	[K]	35.743	35.743
$\epsilon_H/k_B$	[K]	15.950	–
$\epsilon_F/k_B$	[K]	–	30.982
$\sigma_C$	[Å]	3.6316	3.6316
$\sigma_H$	[Å]	2.3291	–
$\sigma_F$	[Å]	–	2.8527
$q_C$ [11]	[e]	–0.153	0.120
$\angle_{C-C}$ [11]	[Å]	1.390	1.393
$\angle_{C-H}$ [11]	[Å]	1.082	–
$\angle_{C-F}$ [11]	[Å]	–	1.322
$\rho_c^{\text{sim}}$	[g/cm <sup>3</sup> ]	0.3062 ± 0.0011	0.5852 ± 0.0041
$\rho_c^{\text{exp}}$ [14]	[g/cm <sup>3</sup> ]	0.3090	0.5552
$T_c^{\text{sim}}$	[K]	561.30 ± 1.37	517.43 ± 1.46
$T_c^{\text{exp}}$ [14]	[K]	562.05	516.73
$P_c^{\text{sim}}$	[bar]	53.9	30.6
$P_c^{\text{exp}}$ [14]	[bar]	48.9	33.0
$C$		$4.76 \cdot 10^{-4} \pm 7.6 \cdot 10^{-6}$	$8.40 \cdot 10^{-4} \pm 3.5 \cdot 10^{-5}$
$\beta$		0.3025 ± 0.0058	0.2834 ± 0.0132
$B_0$		0.1603 ± 0.0051	0.3370 ± 0.0231

The parameters of fitting GEMC data to Eqs. (2) and (3) are also presented.

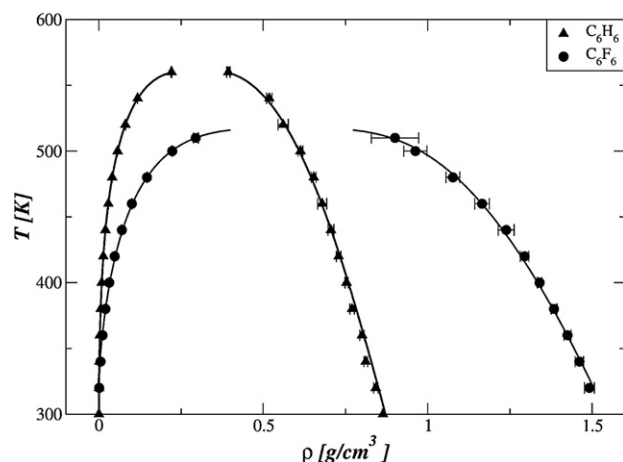


**Fig. 2.** The liquid–vapor coexistence curve predicted by GEMC simulations, using the proposed in this work potential models for  $C_6H_6$  and  $C_6F_6$  (points). In the case of  $C_6H_6$  the available experimental data (line) [14] are presented. For  $C_6F_6$  the fitted densities (line) are presented.

systematically examined by performing subsequent extended verification runs. These simulations were performed using 512 molecules in and simulation length of 1 ns. The results obtained from these simulations are presented in Fig. 1b. From this figure we may clearly see that the calculated pressure using the new models is in excellent agreement with experiment in the whole range of temperatures and densities.

Furthermore, the optimized models were examined in respect to their reliability in predicting the critical parameters of benzene and hexafluorobenzene. To do so, we performed Gibbs Ensemble Monte Carlo (GEMC) simulations [17], to calculate the  $\rho$ – $T$  vapor–liquid coexistence envelope. In the GEMC calculations, 432 molecules were used, performing composite translation–rotation and volume exchange moves, with relative probability 999:1 and for  $10^7$  moves. For each state point, an initial equilibration run of  $10^6$  steps with only translation–rotation moves was performed for the two simulation boxes. Initial box dimensions correspond to experimental liquid and vapor densities for benzene and approximate densities for hexafluorobenzene since, to our knowledge, experimental liquid–vapor coexistence densities are not available in the literature. Then, the GEMC method was used with this configuration as the initial one. All Monte Carlo calculations were performed with the Towhee package [18]. The obtained liquid and vapor densities along the coexistence curve are presented in Fig. 2. Using these results, the critical temperature and density were estimated using the rectilinear diameter law, as described in the following equations:

$$\frac{\rho_l + \rho_v}{2} = \rho_c + C(T_c - T) \quad (2)$$

$$\rho_l - \rho_v = B_0(T_c - T)^\beta + B_1(T_c - T)^{\beta + \Delta} + B_2(T_c - T)^{\beta + 2\Delta} + \dots \quad (3)$$

The resulting critical parameters from fitting Eqs. (2) and (3) to the GEMC data are presented in Table 1. We must note that fitting of Eq. (3) in GEMC data produces very small values for parameters  $B_1$ ,  $B_2$  and as a result high uncertainties for parameter  $\Delta$ . Thus, the fit was performed using only the first term in Eq. (3). The critical pressure for GEMC simulations was evaluated by fitting the simulated vapor pressure with Clausius–Clapeyron equation and extrapolation at the predicted critical temperature. The critical pressure obtained is also presented in Table 1. From data in Table 1 it seems that the proposed potential models are accurate in predicting the critical parameters of both systems. Taking thus into account the fact that the optimized potential models reproduce accurately the P,V,T phase space of both systems at liquid, vapor–liquid equilibrium and SC state points, we

calculated also structural properties of the systems at state points where experimental data are available. Both systems have been studied experimentally at liquid conditions using neutron diffraction techniques [11,15,19]. In these cases the total neutron weighted pair radial distribution function (prdf)  $g_{inter}(r)$  has been measured in terms of the atom-atom prdfs in each system. In the case of benzene, this function is expressed in terms of the C–C, C–H and H–H atom prdfs using the relation [11]:

$$g_{inter}(r) = 0.25 \cdot g_{CC}(r) + 0.25 \cdot g_{HH}(r) + 0.50 \cdot g_{CH}(r) \quad (4)$$

For hexafluorobenzene, this function is expressed in terms of the C–C, C–F and F–F atom-atom prdfs [11]:

$$g_{inter}(r) = 0.29 \cdot g_{CC}(r) + 0.21 \cdot g_{FF}(r) + 0.50 \cdot g_{CF}(r) \quad (5)$$

The functions  $g_{inter}(r)$  were calculated using the optimized potential models at the same state points with experiment and they are presented in comparison with the experimental ones in Fig. 3. From this figure we can observe that in the case of benzene the agreement between the calculated and experimental  $g_{inter}(r)$  is

excellent in a wide range of thermodynamic state points, from ambient conditions up to supercritical ones (573 K). Comparing the total radial distribution functions for  $C_6H_6$  obtained using the potential model proposed in this work with the corresponding obtained using the Williams potential [11,19], we may observe that the proposed potential model is in better agreement with experimental data, especially at short distances. In the case of hexafluorobenzene we may observe that the calculated  $g_{inter}(r)$  reproduces the features of the experimental one, exhibiting only a small difference in the estimation of the first peak intensity, located at 5.7 Å, both at room temperature and close to the boiling point.

Taking into account all the previously discussed issues, we may conclude that the optimized potential models presented in this study reproduce the thermodynamic and structural properties of both systems in a wide range of thermodynamic conditions and hence could be generally employed in simulation studies of these fluids.

### 3. Local density inhomogeneities

As it has been previously mentioned, one of the main reasons for developing new potential models for benzene and hexafluorobenzene

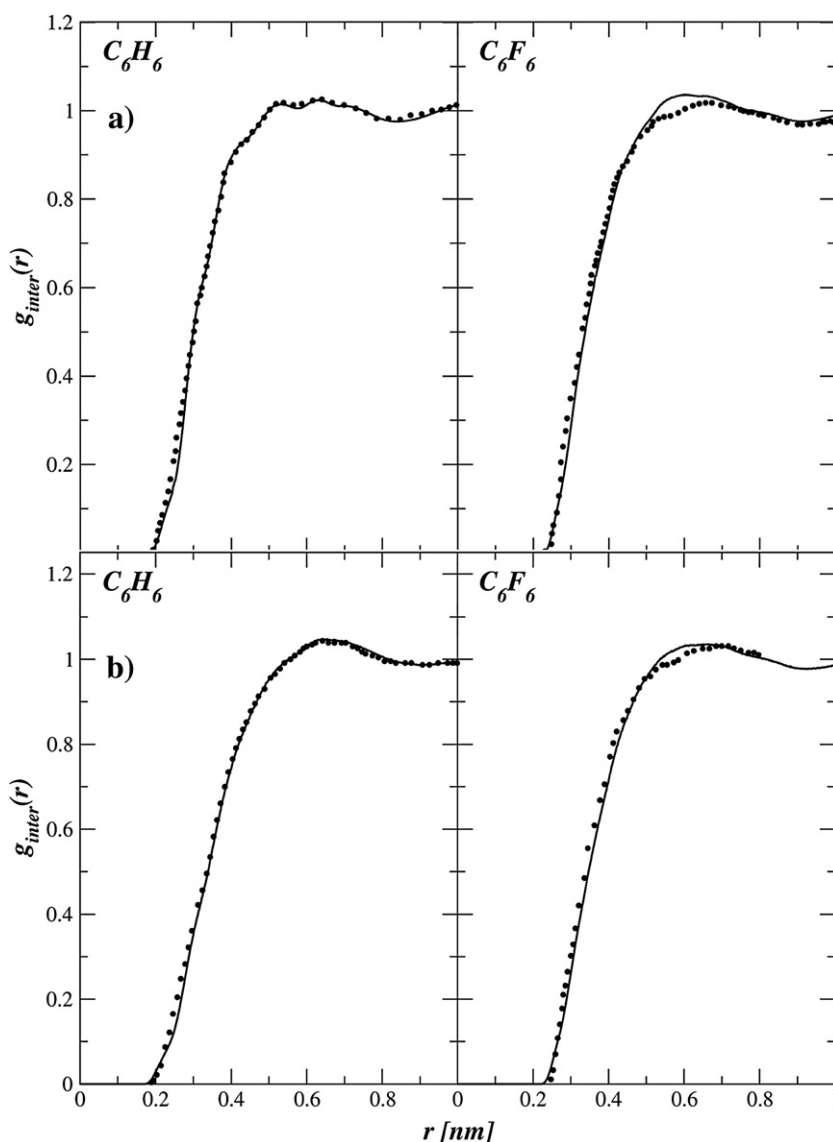


Fig. 3. a) Comparison between the simulated (lines) and experimental (points) [11] total radial distribution functions for  $C_6H_6$  and  $C_6F_6$  at room temperature, using the new optimized potential models. b) Comparison between the simulated (lines) and experimental (points) [11,19] total radial distribution functions for  $C_6H_6$  and  $C_6F_6$  at high temperatures. For  $C_6H_6$ :  $T = 573$  K,  $\rho = 0.573$  g/cm<sup>3</sup> [19]. For  $C_6F_6$ :  $T = 350$  K,  $\rho = 1.483$  g/cm<sup>3</sup> [11].

was to investigate the properties of these systems at SC conditions. More specifically, we focused on the investigation of local density inhomogeneities (LDI) in these SC fluids and their corresponding dynamic behavior. In previous publications we have extensively signified the effects of LDI on the characteristic physicochemical properties of SC fluids and tried to investigate the parameters related with their static and dynamic behavior for several categories of SC solvents [7–9]. Therefore, by employing the same methodologies used in previous treatments we calculated the effective local densities,  $\rho_{eff,l}$  [7–9,20], and subsequently the local density augmentation (LDA), ( $\Delta\rho_{eff,l} = \rho_{eff,l} - \rho$ ), and enhancement (LDE), ( $\rho_{eff,l}/\rho$ ), factors, respectively ( $\rho$  is the bulk density). The reference density for the calculation of  $\rho_{eff,l}$  is  $2\rho_c$ , since above this value the behavior of the local coordination number as a function of the bulk density is linear [7–9]. The simulations were performed at state points along an isotherm close to the critical temperature of each system ( $T_r = T/T_c = 1.02$ ). We have to note also that along this SC isotherm some experimental measurements for hexafluorobenzene have been quite recently reported [21]. The calculated LDA and LDE values for the first and second solvation shell of both fluids are depicted in Fig. 4. Note that the lines in this figure represent the fitted Weibull (in the case of the LDA)

$$\frac{\Delta\rho_{eff,l}}{\rho_c} = a \left( \frac{c-1}{c} \right)^{(1-c)/c} \left[ \frac{\rho - \rho_0}{b} + \left( \frac{c-1}{c} \right)^{1/c} \right]^{(c-1)} \times \exp \left\{ - \left[ \frac{\rho - \rho_0}{b} + \left( \frac{c-1}{c} \right)^{1/c} \right]^c + \frac{c-1}{c} \right\} \quad (6)$$

and sigmoidal Boltzmann (in the case of LDE)

$$\frac{\rho_{eff,l}}{\rho} = 1 + \frac{a' - 1}{1 + e^{(\rho - \rho_0')/b'}} \quad (7)$$

functions, which according to our previous findings [7,8] have been found very accurate in reproducing the shape of these curves. The parameters of the fitting functions in each case are presented in Table 2. According to these results the LDA and LDE values are more pronounced in the case of hexafluorobenzene and are maximized in the bulk density region 0.7–0.9  $\rho_c$ . These peaks in the LDA curves have been also observed in, more or less, the same bulk density region for a significant number of investigated systems [7–9,20,22,23]. However, the calculated LDA values are lower in comparison with the experimental reported ones for hexafluorobenzene. In a previously reported experimental study Cabaco et al [21] have studied the density dependence of the band center position of the  $\nu_1(A_{1g})$

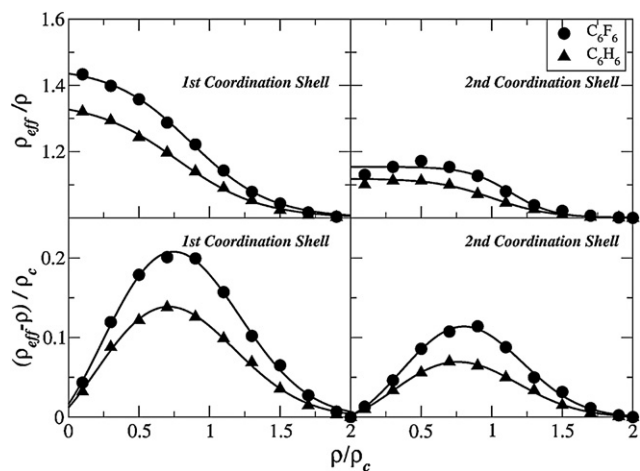


Fig. 4. The calculated LDA and LDE values for the first and second solvation shell of  $C_6F_6$  and  $C_6H_6$ . Lines represent the fitted Weibull (LDA) and sigmoidal Boltzmann (LDE) functions.

Table 2

The fitted parameters of the Weibull and sigmoidal Boltzmann functions (Eqs. (6) and (7)) of benzene and hexafluorobenzene, obtained in the framework of the present study.

Weibull parameters	Benzene		Hexafluorobenzene	
	First shell <sup>a</sup>	Second shell <sup>a</sup>	First shell <sup>b</sup>	Second shell <sup>b</sup>
<i>a</i>	0.138	0.069	0.208	0.114
<i>b</i> / $\rho_c$	1.010	1.003	1.045	1.028
<i>c</i>	2.325	2.542	2.407	2.675
$\rho_0/\rho_c$	0.711	0.761	0.746	0.802
Sigmoidal Boltzmann parameters	Benzene		Hexafluorobenzene	
	First shell	Second shell	First shell	Second shell
<i>a'</i>	1.351	1.119	1.455	1.154
<i>b'</i> / $\rho_c$	0.295	0.206	0.278	0.151
$\rho_0'/\rho_c$	0.770	0.771	0.869	1.132

<sup>a</sup> For benzene the first and second shell cut-offs are 8.18 and 13.64 Å, respectively.

<sup>b</sup> For hexafluorobenzene the first and second shell cut-offs are 9.04 and 15.12 Å, respectively.

“breathing” mode of hexafluorobenzene using Raman spectroscopic techniques along the sc isotherm of  $T_r = T/T_c = 1.02$  and in a wide range of densities. By analyzing these results Cabaco et al obtained the local densities and corresponding LDA values for hexafluorobenzene. They have also estimated the LDA values using a different analysis, by investigating the density dependence of the reorientational correlation time of the main symmetry axis of the molecule, which can be extracted from the full width at half-height of the anisotropic and isotropic Raman spectral profiles [21]. In general, we may notice that the maximum LDA value estimated from these Raman spectroscopic measurements is located in, more or less, the same bulk density of  $C_6F_6$  as in the case of our simulation results, exhibiting however higher amplitudes ( $(\Delta\rho_{eff,l}/\rho_c)_{max} \approx 0.8-1.0$ , see Fig. 3 in Ref. 21).

At this point we have to note that these systematic discrepancies between simulated and experimental values have been observed and reported in the literature for several systems [8,9,23,24] and the possible reasons responsible for this behavior have been extensively discussed in previous publications [8,9,23]. In general, we may say that a spectroscopic determination of the LDA in SC fluids strongly depends on the selection of the appropriate vibrational mode as a probe used and the methodology employed to analyze spectral shifts and widths [8,9,23,25]. Moreover, the length scale determining the region around a molecule in a fluid cannot be determined accurately in the experiment and therefore the experimental LDA values correspond to a somewhat arbitrary “local” region around a central molecule. On the other hand, in the case of simulations the local region around a molecule can be directly defined using a specific cut-off distance. Therefore, the only parameter affecting the reliability of the results obtained by simulations is the accuracy of the employed potential models in reproducing the local intermolecular structure of the fluids. In the present treatment we have seen that the potential models employed reproduce quite accurately the structure of both fluids, and therefore might be characterized as suitable ones for such kind of structural investigations.

Besides the investigation of the static behavior of LDI in SC benzene and hexafluorobenzene we calculated also the local density reorganization times,  $\tau_{\Delta\rho_l}$ , by integrating the calculated local density time correlation functions  $C_{\Delta\rho_l}(t)$ , where  $\Delta\rho_l(t)$  is the local-density deviation, relative to the mean local one, and is defined as  $\Delta\rho_l(t) = \rho_l(t) - \langle\rho_l\rangle$  [7,8]. A complete discussion on the definitions of these dynamic properties can be found in details in our previous publications [7,8]. In brief, the relaxation time  $\tau_{\Delta\rho_l}$  describes the time scale required for the reorganization of the local environment around a molecule. In Fig. 5a representative 3-dimensional plot depicting the dependence of the calculated  $\tau_{\Delta\rho_l}$  values on the cut-off distance of the local region and also on the bulk density of the system is presented for benzene. According to this figure, the  $\tau_{\Delta\rho_l}$  values depend not only on

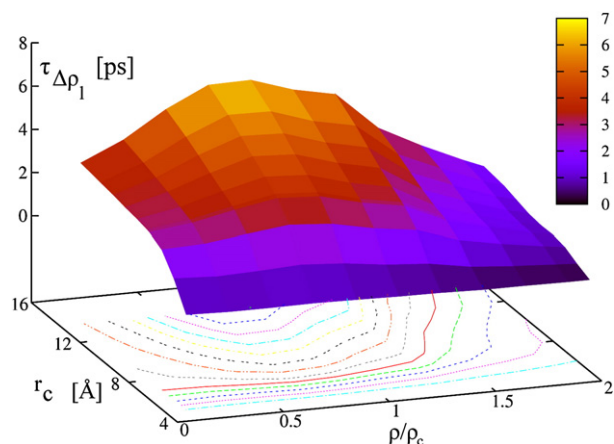


Fig. 5. Dependence of the calculated  $\tau_{\Delta\rho_l}$  on the cut-off radius around a central molecule and on the bulk density for benzene.

the density of the fluid, but also on the length scale of the region taken into account in the calculations. By extending the cut-off distance around a central molecule, the reorganization time exhibits maximum values in the density range where the LDIs become more significant and the LDA values are also maximized. However, this behavior is not apparent at shorter intermolecular distances. All these findings signify that at more extended length scale, the long-range density fluctuations and related collective effects influence differently the local density reorganization mechanisms than at shorter intermolecular distances, where probably direct intermolecular interactions seem to have a more important contribution [8,9,26,27]. The same behavior has been observed also for hexafluorobenzene. Note also that similar conclusions have been reported also for other systems in our previous publications [7–9,27], signifying thus that this behavior is more or less a universal one.

#### 4. Concluding remarks

In the present study, the properties of benzene and hexafluorobenzene have been investigated in a wide range of thermodynamic conditions by employing molecular dynamics and Monte Carlo simulation techniques. Newly developed optimized potential models have been employed in our study, and their reliability in reproducing several thermodynamic and structural properties of the systems in liquid, vapor–liquid equilibrium and supercritical state points has been systematically verified. The results obtained have revealed that the optimized models are accurate in predicting several properties of the fluids in a very wide range of thermodynamic state points.

Moreover, in the present treatment we focused on the investigation of LDI and related dynamics in both SC fluids, by employing the new optimized potential models in our simulation studies. According to our calculations, the LDA is more pronounced in the case of hexafluorobenzene than in benzene. Concerning the dynamic behavior of LDI, we have calculated the local density time correlation functions  $C_{\Delta\rho_l}(t)$  and the corresponding local density reorganization times  $\tau_{\Delta\rho_l}$  as a function of the bulk density and the cut-off distance around a central molecule. The results obtained have shown that the local density reorganization procedure is affected by the length scale of the region around a central molecule. Therefore by increasing the spherical cut-off around a molecule, due to the contribution of long-range collective critical effects, this time is maximized at the bulk density region where the LDA values are also maximized.

#### References

- [1] M.P. Allen, D.J. Tildesley, Computer Simulation of Liquids, Clarendon Press Oxford, 1987.
- [2] K.E. Gubbins, N. Quirke, Molecular Simulation and Industrial Applications (Topics in Molecular Simulation), Taylor and Francis, 1997.
- [3] D. Frenkel, B. Smit, Understanding Molecular Simulation: From Algorithms to Applications, Academic Press, 1996.
- [4] C.A. Eckert, B.L. Knutson, P.G. Debenedetti, Nature 383 (1996) 313.
- [5] M. Besnard, T. Tassaing, Y. Danten, J.M. Andanson, J.C. Soetens, F. Cansell, A. Loppinet-Serani, H. Reveron, C. Aymonier, J. Mol. Liq. 125 (2006) 88.
- [6] S.C. Tucker, Chem. Rev. 99 (1999) 391.
- [7] I. Skarmoutsos, J. Samios, J. Phys. Chem. B 110 (2006) 21931.
- [8] I. Skarmoutsos, J. Samios, J. Chem. Phys. 126 (2007) 044503.
- [9] I. Skarmoutsos, D. Dellis, J. Samios, J. Phys. Chem. B 113 (2009) 2783–2793.
- [10] W.L. Jorgensen, D.L. Severance, J. Am. Chem. Soc. 112 (1990) 4768.
- [11] M.I. Cabaco, Y. Danten, M. Besnard, Y. Guissani, B. Guillot, J. Phys. Chem. B 101 (1997) 6977.
- [12] M.D. Elola, B.M. Ladanyi, J. Chem. Phys. 122 (2005) 224508.
- [13] W. Lemmon, M. McLinden, D. Friend, Thermophysical Properties of Fluid Systems in NIST Chemistry WebBook, NIST Standard Reference Database Number 69, Eds. P.J. Linstrom and W.G. Mallard, National Institute of Standards and Technology, Gaithersburg MD, 20899, June 2005 (<http://webbook.nist.gov>).
- [14] D. Hogenboom, K. Krynicki, D.W. Sawyer, Mol. Phys. 40 (1980) 823.
- [15] Y. Danten, M.I. Cabaco, T. Tassaing, M. Besnard, J. Chem. Phys. 115 (2001) 4239.
- [16] B. Hess, C. Kutzner, D. van der Spoel, E. Lindahl, J. Chem. Theory Comput. 4 (2008) 435.
- [17] A.Z. Panagiotopoulos, Mol. Phys. 61 (1987) 813.
- [18] Available at <http://towhee.sourceforge.net>.
- [19] T. Tassaing, M.I. Cabaco, Y. Danten, M. Besnard, J. Chem. Phys. 113 (2000) 3757.
- [20] W. Song, R. Biswas, M. Maroncelli, J. Phys. Chem. A 104 (2000) 6924.
- [21] M.I. Cabaco, M. Besnard, T. Tassaing, Y. Danten, Pure Appl. Chem. 76 (2004) 141.
- [22] S. Nugent, B.M. Ladanyi, J. Chem. Phys. 120 (2004) 874.
- [23] W. Song, M. Maroncelli, Chem. Phys. Lett. 378 (2003) 410.
- [24] M.I. Cabaco, S. Longelin, Y. Danten, M. Besnard, J. Phys. Chem. A 111 (2007) 12966.
- [25] M.I. Cabaco, M. Besnard, T. Tassaing, Y. Danten, J. Mol. Liq. 125 (2006) 100.
- [26] M.W. Maddox, G. Goodyear, S.C. Tucker, J. Phys. Chem. B 104 (2000) 6266.
- [27] I. Skarmoutsos, E. Guardia, J. Phys. Chem. B 113 (2009) 8887.